Environmental Science & Technology

Article

pubs.acs.org/est

Dissolved Nitrous Oxide Concentrations and Fluxes from the Eutrophic San Joaquin River, California

Sarra E. Hinshaw* and Randy A. Dahlgren

Land, Air and Water Resources, University of California, Davis, One Shields Avenue, Davis, California 95616, United States

Supporting Information

ABSTRACT: Agriculturally impacted ecosystems can be a source of the greenhouse gas, nitrous oxide (N_2O); yet in situ measurements of N_2O fluxes are sparse, particularly in streams and rivers. Dissolved N_2O was measured from 9 sites over a 13-month period and a gas exchange model was used to predict N_2O fluxes. N_2O fluxes were measured at 4 sites on 7 sampling dates using floating chambers. In addition, dissolved N_2O in porewaters was measured at 4 sites at various depths from 2 to 30 cm. Dissolved N_2O–N concentrations in surface waters (0.31–1.60 $\mu g\ L^{-1}$) varied seasonally with highest concentrations in late fall and early summer and lowest in winter. Estimated N_2O–N fluxes (26.2–207 $\mu g\ m^{-2}\ hr^{-1}$) were in relative agreement with measured N_2O fluxes using floating chambers (9.5–372 $\mu g\ m^{-2}\ hr^{-1}$) and correlated strongly with temperature and nitrate concentrations (R^2 = 0.86). Maximum dissolved N_2O–N:NO_3^-–N ratios were higher in sediment-porewaters at 0.16, compared to surface waters (0.010). The calculated EF5-r value (mean = 0.0028; range = 0.0012–0.0069) was up to 3 times greater than the current IPCC EF5-r emissions factor (0.0025 kg N_2O–N emitted per kg of NO_3^-–N leached). The highest EF5-r values were found in the high-flow sampling events when dissolved N_2O and NO_3^- concentrations were low, highlighting potential constraints in the IPCC methodology for large rivers.

INTRODUCTION

Nitrous oxide (N_2O) is a potent greenhouse gas having a global warming potential 298 times greater than carbon dioxide over a 100-yr period.[1] Agricultural N_2O emissions associated with nitrogen fertilizer use are considered the main source of global N_2O emissions (19 Tg N yr^{-1}), with an estimated 5.3 Tg N yr^{-1} originating from agricultural soils.[2] Indirect N_2O emissions contribute 0.4 Tg N yr^{-1} from denitrification of nitrate originating from leaching and runoff processes.[3]

The current IPCC method for estimating N_2O emissions associated with leaching and runoff of nitrogen (N) multiplies the mass of fertilizer and manure N lost from agricultural systems (NLEACH; kg NO_3^-–N) by the emissions factor EF5 or N_2O yield (kg N_2O–N per kg NO_3^-–N leached). The current EF5 value of 0.0075 kg N_2O–N per kg NLEACH includes N_2O emissions from groundwater and surface drainage (EF5-g), rivers (EF5-r), and estuaries (EF5-e), with each component contributing 0.0025 kg N_2O–N per kg NLEACH.[4]

The current EF5-r value was revised from 0.0075[5] to 0.002 [4] and is based on data primarily from small river systems, but there remains great uncertainty in scaling these values to larger rivers.[6−8] While several studies have used dissolved N_2O and air–water exchange models to estimated N_2O fluxes,[9−12] there are a minimal number of studies that have measured N_2O fluxes directly from streams and rivers (e.g., 13–17). Most of the studies on N_2O from aquatic systems have been performed in small first- or second-order streams over relatively short time periods. A study examining 72 streams found that N_2O fluxes were ∼3 times higher than the revised EF5-r value,[18] whereas Clough et al.[12] found values similar to the revised EF5-r value.

Aquatic ecosystems can be a significant source of N_2O emissions with nitrification and denitrification considered the two main processes producing N_2O.[19] Denitrification is an anaerobic respiration process that reduces NO_3^- to dinitrogen gas (N_2), with N_2O as the intermediate gas product.[20] Nitrification, an aerobic microbial process, oxidizes ammonium (NH_4^+) to NO_3^-, in which N_2O is formed as a byproduct.

Within the agriculturally dominated Central Valley of California, nitrate concentrations in the San Joaquin River (SJR) are highest in the summer dry season (1–4 mg NO_3^-–N L^{-1}). During the dry season, low river flows result in less dilution capacity and lower oxygen concentrations while considerable NO_3^- is delivered to the river by irrigation return flows.[21] Past studies examining groundwater inputs into the SJR suggested that the riparian and hyporheic zones act as an anoxic barrier to NO_3^- transport resulting in little NO_3^- input from regional groundwater sources.[22] River bed sediments generally became anoxic within ∼10 cm, creating favorable conditions for denitrification of NO_3^- mixing into the hyporheic zone from surface waters. In spite of the strong evidence for denitrification potential in the

Received: April 6, 2012
Revised: December 19, 2012
Accepted: December 23, 2012
Published: December 23, 2012

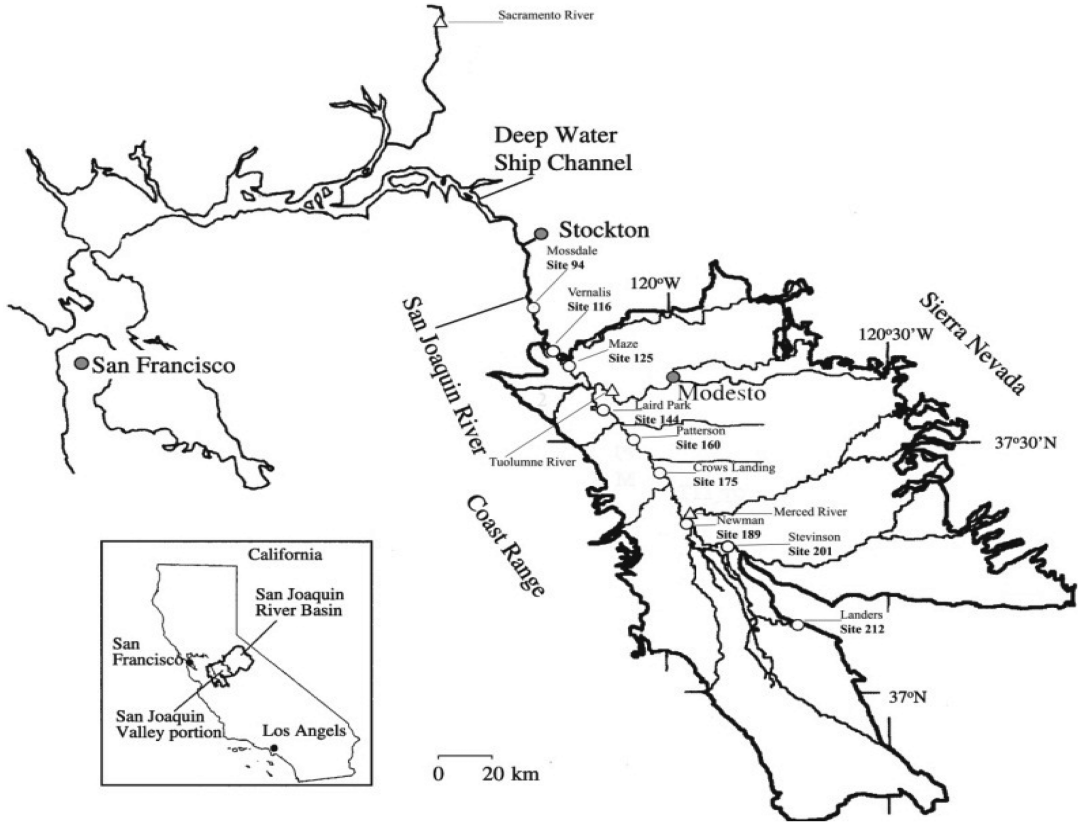

Figure 1. Location of study sites. Circles represent the 10 main sites on the San Joaquin River. Triangles represent Merced, Tuolumne, and Sacramento Rivers.

SJR, no studies have directly assessed denitrification or N_2O emissions from this river system.

In this study, we built upon these past findings by measuring temporal and spatial patterns in N_2O fluxes over a 118-km reach of the SJR and selected tributaries for a 13-month period. The primary objectives of this study were to assess (i) seasonal and temporal variations in dissolved N_2O concentrations, (ii) measure N_2O fluxes from surface water using floating chambers, (iii) estimate N_2O fluxes using a water−air gas exchange model, (iv) relate measured and estimated N_2O fluxes to environmental factors (e.g., NO_3^- concentration, temperature, flow), and (v) compare EF5-r values measured in the SJR with the IPCC estimates (EF5-r[4]). Results of this study provide the first information available for N_2O emissions from agricultural rivers in the Central Valley of California. These data provide new information for understanding nitrogen cycling processes in riverine systems and further our knowledge for developing management strategies for reducing N_2O emissions from agricultural watersheds.

MATERIALS AND METHODS

The study was conducted along the SJR and its tributaries located in the Central Valley of California. Nine sampling sites were located over a 118-km reach of the lower SJR from Lander to Mossdale (Figure 1). The study area has a Mediterranean climate with hot, dry summers (mean summer temperature of 24 °C) and cool, moist winters (mean winter temperature of 8 °C; mean annual precipitation ranging from 254 to 305 mm). The river drains 19 024 km^2, of which 11 135 km^2 are from the Sierra Nevada, 5812 km^2 are from the San Joaquin Valley and 2077 km^2 are from the Coast Ranges. The SJR within the study area has a mean depth of 2 m (range = 0.5−6 m), and a low gradient (~0.0156%) with a sandy substratum.[23] Approximately 79% of the average river flow in the SJR comes from east-side river basins originating in the Sierra Nevada: Merced River (17%), Tuolumne River (28%), and Stanislaus River (34%[21]). The remainder originates as surface and subsurface drainage from irrigated agriculture. Agricultural diversions and drains cycle water along the entire length of the lower SJR. Agricultural drains are estimated to contribute up to 90% of the annual NO_3^- load.[24] The surrounding land mostly comprises dairy farms, pasture, wetlands, orchard crops, and row crops. The only major sewage input along the study reach is from the City of Modesto Waste Water Treatment Plant located on the east side of the river alongside Site 160. Secondary treated wastewater flows to surrounding cropland fields adjacent to the river study site and directly into the SJR at 96 528 m^3 d^{-1}.[25] Common aquatic macrophytes are present along the river banks during low flow periods, including hyacinth (*Eichhornia crassipes*), pennywort (*Hydrocotyle umbellate*), and primrose (*Ludwigia* spp.) Additional information on the SJR and its watershed can be found in Kratzer et al.[21] and Zamora et al.[22]

To measure dissolved N_2O in surface waters, samples were collected midstream from 9 sites as defined by river distance, with river kilometer Site 212 and Site 94 being the upstream and downstream sites, respectively. Samples were collected 10 times between October 2010 and September 2011 to ensure sampling covered differences in season and variable river flow. In addition to the 9 sites located on the SJR, samples were collected on 7 sampling dates from two SJR tributaries (Merced and Tuolumne Rivers) and from the Sacramento River (SAC). Replicate surface water samples from the top ~5 cm were placed in 20-mL Wheaton crimp-top headspace vials with straight plug

dx.doi.org/10.1021/es301373h | *Environ. Sci. Technol.* 2013, 47, 1313−1322

rubber stoppers, preserved with 6 drops of $ZnCl_2$ (50% v/w), and stored at 4 °C through completion of analysis.[26] Sampling took place primarily between 10:00 and 16:00 h to minimize potential discrepancies due to diurnal variations. To assess diurnal variability, paired samples were collected from four sites at 09:00 and 21:00, in April, May, and June 2011. Significant differences were not found in nitrate−N, dissolved O_2 (DO), and N_2O−N concentrations which differed by 0.07 mg L^{-1} (0.02%); 0.13 mg L^{-1} (0.01%), and 0.09 μg L^{-1} (0.01%), respectively (paired t test, $P > 0.05$).

The headspace equilibrium technique was used to measure dissolved N_2O concentrations. Six mL of water was removed from the 20-mL vials and the headspace was replaced with ultrahigh-purity helium. Vials were placed on a shaker table for 1 h to equilibrate gas and liquid phases. Headspace gas was quantified using a gas chromatograph (HP/Agilent 6890, μECD using 10% CH_4 in Ar as the carrier gas). Dissolved N_2O concentrations were calculated using appropriate Bunsen and solubility coefficients to correct for temperature and salinity.[27]

N_2O fluxes were measured from four sites (201, 189, 175, and 160) in August and September 2010 and January, May, July, August, and September 2011 using floating chambers.[28] Chambers consisted of 30 × 30 cm polyurethane containers. Foam was attached around the sides of the containers and they were inserted into the river at a depth of 5 cm with a height of 25 cm, for a resulting headspace of 15.6 L. A three-way valve was sealed to the top of the chamber to allow direct headspace gas sampling during low flows. Three replicate chambers were deployed on an unrestrained rope across the river width during low-flow season (August and September 2010 and 2011) to minimize disturbance between the boundary layers. During high-flow sampling events, chambers were extended a minimum of 2 m from the river bank and drifted with the river current. The chambers were white to minimize heating of headspace gas. Tubing (void volume, 19.8 mL) was attached to the top of the chamber so gas samples could be collected from the river bank. Twenty mL of air was removed from the chamber and expelled as waste during high-flow periods. Using a 30-mL syringe, 15-mL samples were collected and injected into pre-evacuated 12-mL Labco vials every 15 min for 1 h. Nitrous oxide fluxes were calculated as the slope of the linear regression of N_2O concentration versus time (slopes were well fit by a linear regression: $r^2 > 0.95$).

Flux chamber measurements of N_2O from all sites and months were unattainable due to inaccessibility to downstream sites and periodic flooding. Therefore, the dissolved N_2O concentrations were used to estimate N_2O fluxes using model-based estimates of gas exchange. Estimated N_2O fluxes between the water−air interface were calculated from the dissolved N_2O concentrations using[17]

$$F_{N_2O} = V_{tot}(C_w - C_a/K'_H) \quad (1)$$

where F_{N_2O} is N_2O flux (mole m^{-2} s^{-1}), C_w is N_2O concentration (mol m^{-3}) in surface water, C_a is N_2O concentration in air, and K'_H is the dimensionless Henry's Law constant. V_{tot} is the combined gas transfer velocity of N_2O that contains both wind speed and water turbulence. The following equations were used to calculate water turbulence, $V_{benthic}$ (eq 2), and wind turbulence, V_{wind} (eq 3).

$$V_{benthic} = \sqrt{\frac{DU}{h}} \quad (2)$$

$$V_{wind} = 2.78E^{-6}ku^2\left(\frac{Sc}{600}\right)^n \quad (3)$$

The water turbulence was calculated using the river water velocity (U, m s^{-1}), average depth (h, m), and N_2O diffusion coefficient (D, m s^{-1}) (Table 1 and Table S1 in the Supporting Information (SI)). The wind turbulence was calculated using 2.78×10^{-6} as the conversion factor from cm h^{-1} to m s^{-1}, k is a constant (0.31), u^2 is average wind speed adjusted to 10 m (SI eq 6), Sc is the Schmidt number for N_2O defined by the ratio between kinematic viscosity and N_2O diffusion coefficient, and n was calculated as either $^2/_3$ for wind speeds <3.6 m s^{-1} or $^1/_2$ for wind speeds >3.6 m s^{-1}.[29,30]

The following methods were used to calculate the emissions factor EF5-r according to the IPCC assumption that 0.0025 kg N_2O−N evolves from 1 kg of NO_3^-−N leached.[4] Mass of N loss as N_2O was estimated monthly based on nitrate loads, river wetted surface area, flow, and estimated N_2O fluxes for each of the 9 sites. Each variable was calculated for the 9 river reach sections separately by averaging the central site with its adjacent upstream and downstream sites. The river wetted surface area and length were calculated as half the distance above and below each adjacent site (+3 km for Sites 212 and 94). The NO_3^- load moving through the system was calculated from surface water concentrations and flow values. The assumption was made that the mass of NO_3^- leaving the system was from N leached.

A third approach measured the contribution of dissolved N_2O from benthic sediments at sites 201, 189, 175, and 160 from June to August 2010. Porewater was collected from six cross-sectional positions (0, 20, 40, 60, 80, and 100% river width) and at five depths (2−3, 7−8, 12−13, 17−18, and 30 cm). Samples at depths above 18 cm were collected with mini-piezometers[31] while samples from the 30-cm depth were collected with a temporary drive point.[22] N_2O concentrations were analyzed as described above.

In-situ measurements of dissolved oxygen (DO), pH, electrical conductivity (EC, μS cm^{-1}), and temperature (°C) were taken using a YSI 556 multiprobe. Wind speed and discharge were obtained from the California Irrigation Management Information System[32] and California Data Exchange Center, respectively.[33] River depth, width, and velocity were calculated based on Brown.[34] Further, a 60-mL sample of surface and sediment-porewaters was collected and analyzed within 48 h for selected water quality constituents. Samples were field-filtered with a prerinsed 0.45-μm nylon syringe filter (Millipore) and stored at 4 °C through completion of analyses. Dissolved organic carbon (DOC) samples were acidified with HCl in the field to pH <2. The vanadium chloride method was used to spectroscopically determine NO_3^-−N.[35] Determination of NH_4^+−N was made spectroscopically using a salicylate analog of indophenol blue.[36] DOC was measured by ultraviolet-enhanced persulfate digestion and infrared detection (Phoenix 8000; Teledyne Tekmar).

Data normality was determined using the Shapiro−Wilk test. When necessary, data were log or log+1 transformed to meet normality assumptions. Two-way ANOVA's were used to detect seasonal and spatial patterns in dissolved N_2O concentrations, N_2O percent saturation, and estimated N_2O fluxes over the 13-month period. Two-way ANOVA's were used to test for seasonal differences in flux chamber measurements of N_2O and spatial differences among the four sites. Two-way ANOVA was used to detect spatial patterns in N_2O sediment-porewater with depth and site as main effects. Pearson's correlation was used to examine the

correlation between independent environmental variables. Piecewise regression was used to investigate thresholds controls on N_2O. Simple and multiple linear regressions were utilized to assess correlations between N_2O and water quality constituents and Spearman's correlation was used to test for nonlinear correlations.[37] All statistical analyses were performed in SPSS 14.[38]

RESULTS

River and water quality characteristics for the study period are provided in Table 1. River discharge varied greatly among sampling sites and dates ranging from 4.1 to 787 $m^3\ s^{-1}$ with highest flows at downstream sites and during the snowmelt period in March–April (Figure 2). Water temperatures ranged seasonally from 8.9 to 28.4 °C. DO ranged from 45% to 110% of saturation (4.0–10.8 mg L^{-1}) and correlated negatively with water temperature ($r = -0.49$, $p < 0.001$). The pH values were

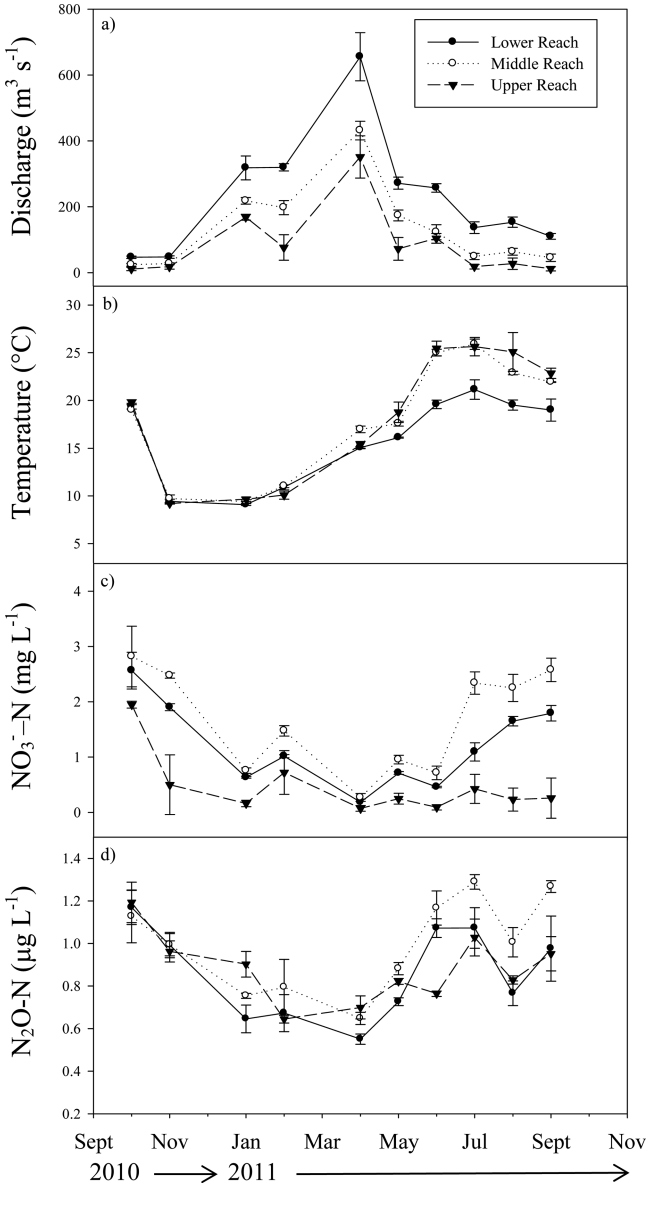

Figure 2. Plots of mean (a) discharge, (b) temperature, (c) nitrate concentrations, and (d) dissolved N_2O concentrations for upper reach (sites 212, 201, and 189), middle reach (sites 175, 160, 144), and lower reach (sites 125, 116, 94). (Error bars represent SE, $n = 6$).

Table 1. Range, Mean, and SD[a] of River Characteristics

site	temperature (°C)			discharge ($m^3\ s^{-1}$)			NO_3^-–N (mg L^{-1})			DOC (mg L^{-1})			DO (mg L^{-1})			N_2O ($\mu g\ L^{-1}$)			$\%N_2O$			N_2O saturation			velocity (ms^{-1})		
	range	mean	SD	range	mean	SD	range	mean	SD	range	mean	SD	range	mean	SD	range	mean	SD	range	mnean	SD	range	mean	SD	range	mean	SD
212	9.3–27.3	19.2	7.2	4–249	71	88	0.11–1.39	0.47	0.44	3.2–9.0	5.5	1.7	4.5–8.5	6.7	1.3	0.50–1.11	0.74	0.2	0.045–1.01	0.31	0.30	206–413	322	17	0.26–0.71	0.47	0.15
201	9.8–27.3	19.3	7.2	5–334	73	106	0.05–2.75	1.06	1.02	2.7–8.8	5.1	1.8	4.6–9.9	6.9	1.6	0.47–0.98	0.76	0.2	0.031–0.92	0.25	0.32	209–448	334	17	0.35–1.10	0.69	0.20
189	9.2–24.2	17.2	5.9	17–470	124	137	0.13–2.83	1.17	0.93	1.6–7.1	4.0	1.7	4.0–9.4	7.1	1.6	0.42–1.60	0.92	0.4	0.025–0.45	0.17	0.15	187–621	388	34	0.32–0.86	0.68	0.14
175	9.3–25.8	17.8	6.2	18–450	127	132	0.26–2.50	1.34	0.77	2.0–7.5	5.3	1.8	5.9–8.8	7.4	1.1	0.55–1.40	0.92	0.3	0.025–0.31	0.11	0.09	218–699	414	35	0.37–1.09	0.75	0.19
160	9.2–27.1	17.9	6.4	22–380	118	116	0.39–3.50	1.75	1.05	2.4–8.2	5.7	1.9	6.4–8.8	7.5	0.8	0.60–1.35	0.96	0.3	0.033–0.17	0.08	0.05	236–442	429	36	0.18–0.90	0.46	0.23
144	9.4–25.2	18.1	5.9	31–473	157	136	0.15–3.22	1.78	1.02	3.0–7.9	5.5	1.7	6.2–9.8	7.6	1.1	0.71 –1.42	1.07	0.2	0.037–0.48	0.11	0.13	276–724	461	32	0.44–1.28	0.78	0.29
125	9.2–23.5	16.6	5.3	37–566	196	159	0.10–3.21	1.35	0.96	2.7–6.4	4.5	1.4	7.1–10.8	8.4	1.2	0.61 –1.23	0.91	0.2	0.037–0.81	0.16	0.23	239–729	424	39	0.37–0.95	0.66	0.21
116	8.9–21.0	15.8	4.6	48–787	260	216	0.12–2.13	1.11	0.67	3.1–6.0	4.6	1.2	6.6–10.6	8.0	1.2	0.50–1.03	0.79	0.1	0.049–0.43	0.12	0.12	235–546	374	26	0.37–0.95	0.64	0.21
94	9.0–20.1	15.8	4.4	50–568	221	158	0.28–2.35	1.17	0.68	2.9–7.0	4.8	1.5	6.6–9.1	7.8	0.8	0.63–1.36	0.88	0.2	0.046–0.26	0.11	0.07	249–584	405	25	0.11–1.04	0.5	0.33
MER	9.0–21.8	17.2	4.7	11–147	64	50	0.13–2.31	0.78	0.96	2.3–4.6	3.3	0.9	6.2–9.4	8.1	1.2	0.42–1.96	0.98	0.5	0.050–0.39	0.28	0.12	43–346	118	112		NA	
TLM	9.8–20.7	15.2	4.8	3–224	104	80	0.05–2.08	0.67	0.84	2.3–4.3	3.3	0.8	9.0–11.0	9.7	1.1	0.45–1.84	1.03	0.6	0.081–1.53	0.57	0.48	45–670	274	344		NA	
SAC	9.0–20.5	16.5	4.0	417–1731	872	446	0.07–0.04	0.17	0.09	1.9–4.6	3.1	0.9	1.4–11.1	7.6	3.0	0.41–0.67	0.55	0.1	0.212–1.13	0.45	0.31	90–621	207	172	0.57–1.44	0.89	0.03

[a]Standard deviation for environmental properties, $n = 11$ for temperature, discharge, NO_3^-–N, DOC, and DO, $n = 22$ for N_2O–N and percent N_2O saturation, $\%\ N_2O$ = ratio of $(N_2O\text{–}N/NO_3^-\text{–}N) \times 100$; concentration of dissolved N_2O–N (mg L^{-1}) divided by the concentration of NO_3^-–N (mg L^{-1}) in the surface water. NA = data not available.

dx.doi.org/10.1021/es301373h | Environ. Sci. Technol. 2013, 47, 1313–1322

similar throughout the year and among sites (range = 7.0–8.5). Nitrate concentrations ranged from 0.05 to 3.5 mg N L^{-1} with concentrations increasing from Site 212 to Site 160 and then decreasing downstream due to dilution from Sierra Nevada tributaries (Figure 2). Ammonium concentrations were below 0.3 mg N L^{-1} for the duration of the study with no statistical differences between seasons or sites. Dissolved organic carbon ranged from 1.6 to 9.0 mg L^{-1}.

Dissolved organic carbon and NO_3^-–N in sediment-porewater ranged from 1.8 to 26.9 (mean = 6.8 mg L^{-1}) and 0.01 to 5.38 mg L^{-1} (mean = 0.60 mg L^{-1}), respectively (Table S1). Nitrate concentrations decreased with depth at all sites and most positions ($p < 0.01$) and were generally <0.05 mg N L^{-1} below 18 cm. Sediment-porewaters below 18 cm at Sites 201 and 189 were considered to be incoming groundwater demonstrated by a 2–3 °C difference in temperature between 18 and 30 cm and distinct increases in EC between the two depths. Dissolved oxygen concentrations ranged from 0.17 to 6.4 mg L^{-1} with a median of 1.0 mg L^{-1}.

Dissolved N_2O–N concentrations in surface waters ranged from 0.31 to 1.60 μg L^{-1} (mean = 0.91 μg L^{-1}) and were supersaturated in all samples. Percent N_2O saturation ranged from 186 to 729% with a median value of 362%. Dissolved N_2O–N and percent saturation were significantly different between months ($P < 0.001$) showing a strong seasonal pattern with lowest concentrations in April and highest concentrations throughout the summer period (June–September) (Table 1, Figure 2). When averaged by site across all sampling dates, dissolved N_2O concentrations and percent saturation followed a pattern similar to NO_3^- concentrations with increasing N_2O concentrations to middle reach sites and decreasing concentrations downstream (Figure 2). The dissolved N_2O–N:NO_3^-–N ratio ranged from 0.0002 to 0.01 with highest ratios found at the most upstream site (Table 1).

Model-estimated N_2O–N fluxes, calculated from dissolved N_2O–N concentrations and model-based estimates of gas exchange, ranged from 26.2 to 207 μg m^{-2} hr^{-1} and varied greatly between months ($P < 0.001$, Figure 3). Lowest fluxes were found in January coinciding with low water temperatures and low NO_3^- concentrations. Similar to dissolved N_2O and NO_3^- concentrations, peak estimated N_2O fluxes were typically found in the middle reach sites (Figure 3). Pooling data across sampling months indicated temperature and NO_3^-–N concentrations best predicted dissolved N_2O–N concentrations ($R^2 = 0.86$, $P < 0.010$) and estimated fluxes ($R^2 = 0.84$, $P < 0.001$).

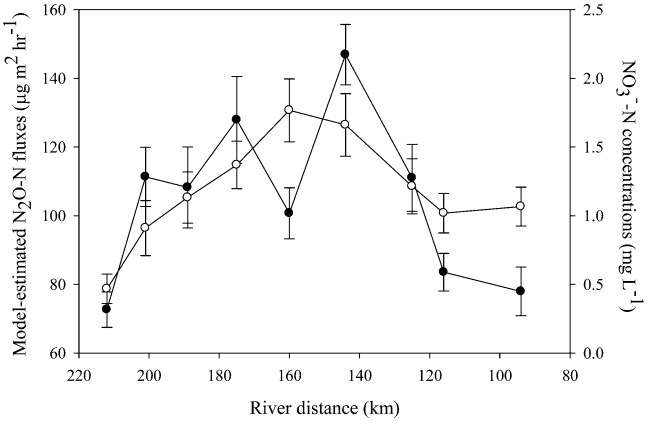

Figure 3. Model-estimated N_2O fluxes (error bars SE, $n = 18$, closed circles) and nitrate concentrations (error bars SE, $n = 10$, open circles) at each site averaged across all sampling months.

Measured N_2O–N fluxes from Site 201 to Site 160 ranged from 9.5 to 372 μg m^{-2} hr^{-1} with a mean of 135 μg m^{-2} hr^{-1} (Figure 4, Table S3). N_2O fluxes correlated with dissolved N_2O concentrations ($r = 0.56$, $p < 0.001$) and exponentially with percent saturation ($r = 0.62$, $p < 0.001$). Flux chamber measurements of N_2O were compared to model-estimated N_2O fluxes from the Sites 201, 189, 175, and 160 during the same sampling month. Measured fluxes were within the standard deviation for the model-estimated fluxes but tended to be higher than estimated values during the summer low-flow period and lower than estimated values during the winter high-flow period (Figure 4). Measured log-transformed N_2O–N fluxes were positively related with NO_3^-–N concentrations ($R^2 = 0.68$, $P < 0.001$, Figure S1), with no improvement in predictability with the addition of other environmental variables.

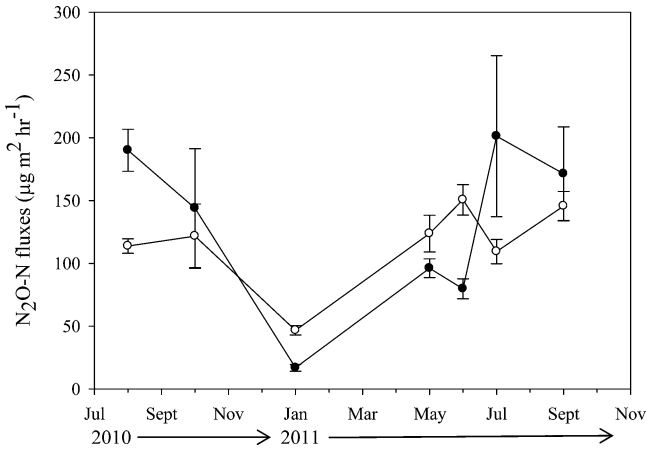

Figure 4. Measured (error bars SE, $n = 8$, closed circles) and model-estimated N_2O fluxes (error bars SE, $n = 12$, open circles). Data for estimated fluxes are shown only for Sites 201, 189, 175, and 160 when N_2O fluxes were measured with floating chambers.

The Tuolumne and Merced Rivers had slightly higher dissolved N_2O–N concentrations, averaging 0.97 (range = 0.45–1.84 μg L^{-1}) and 1.03 μg L^{-1} (range = 0.42–1.96 μg L^{-1}), respectively (Table 1). However, the tributary median NO_3^-–N concentrations (<0.3 mg L^{-1}) were considerably lower than for the main-stem SJR sites. Dissolved N_2O in both tributaries showed seasonal trends parallel to SJR sites and were significantly related to temperature and NO_3^- concentrations ($R^2 = 0.75$, $P < 0.001$). Surface water from the SAC had low N_2O–N (range = 0.4–0.67 μg L^{-1}) and NO_3^-–N concentrations (range = 0.07–0.40 mg L^{-1}) throughout the year (Table 1). In contrast to SJR, dissolved N_2O concentrations from SAC were negatively related to NO_3^- concentrations ($R^2 = 0.37$, $P < 0.02$), but positively related to NH_4^+ concentrations ($R^2 = 0.33$, $P < 0.02$).

Dissolved N_2O–N concentrations in sediment-porewaters ranged from <0.01 to 48.9 μg L^{-1} (mean = 1.52 μg L^{-1}, Figure S2). Below 8 cm, N_2O concentrations were mostly nondetectable, except for Site 189 which showed maximum N_2O concentrations at 30 cm. Dissolved N_2O concentrations in sediment-porewaters were not significantly different between sites or depths (Figure S2). The dissolved N_2O–N:NO_3^-–N ratio ranged from 0.0002 to 1.57 with highest ratios at the upstream site 212 (Table S1).

The river wetted surface area, per site, varied considerably (range = 604 589 to 3 763 295 m^2) with seasonal changes in

dx.doi.org/10.1021/es301373h | Environ. Sci. Technol. 2013, 47, 1313–1322

Table 2. Total Loss of N as N_2O−N kg day^{-1} during Transport from Site 212 to 94 and Mass of NO_3^- Leaving the System at Site 116 Compared to the IPCC Estimates Using EF5-r Value of 0.0025 and NO_3^- −N:N_2O−N kg day^{-1} Ratio Presented as % N_2O for Each Sampling Event from October 2010 to September 2011[a]

month	R.A. km^2[c]	N_2O−N kg day^{-1}	N_2O−N(IPCC)[d]	NO_3^-−N Mg day^{-1}[e]	N_2O %	N_2O−N $\mu g\ L^{-1}$[f]	R. T. hours[g]
Oct.	8.81	27.8	25.3	10.1	0.27	1.16	87
Nov.[b]	11.3	16.5	19.3	7.70	0.21	0.98	83
Jan.	18.1	23.3	41.4	16.6	0.14	0.77	48
Feb.	16.7	33.0	68.8	27.5	0.12	0.70	54
Apr.	25.9	63.4	22.8	9.11	0.69	0.63	47
May	16.0	44.0	41.2	16.5	0.27	0.81	52
Jun.	15.9	43.5	24.8	9.92	0.44	1.00	55
Jul.	10.5	37.5	31.3	12.5	0.30	1.13	71
Aug.	11.8	30.0	52.9	21.2	0.14	0.87	69
Sept.	10.1	31.8	42.2	16.9	0.19	1.07	72
mean	14.5	35.1	37.0	14.8	0.28	0.91	64

[a]The values represent the sum of all 9 sites through the 124 km (+3 km for Site 212 and 94) on the day of sampling, each month. Further information for values at each of the 9 sites can be found in Table S3. [b]Values represent Sites 189−94 only. [c]Total river wetted surface area over the 118 km value from 9 sites (R.A. = River area). [d]IPCC estimated kg N_2O−N emitted per kg NO_3^-−N leached based on EF5-r (0.0025). [e]Calculated NO_3^- loading using NO_3^-−N concentrations and flow data from Site 116. [f]Mean dissolved N_2O concentrations in surface waters. [g]R.T. is residence time of NO_3^-−N through the 124 km (+3 km for Site 212 and 94). Data calculated using wetted surface area, flow data, and NO_3^- concentrations.

river discharge (Table S2). The calculated EF5-r and total N loss as N_2O−N kg day^{-1} were totaled for all 9 river segments (the entire 124 km reach). The cumulative mass of NO_3^-−N transported by the river was calculated for Site 116, the water quality compliance station in the lower SJR, upstream from tidal influence. Daily NO_3^- loads varied greatly by month and site ranging from 7713 to 27 514 kg day^{-1}. Estimated N_2O−N fluxes ranged from 16.5 to 63.4 kg N_2O−N day^{-1} with an annual average of 8.9 kg N_2O−N ha^{-1} yr^{-1} (Table 2, Table S3). The EF5-r factor ranged from 0.0012 to 0.0069 kg N_2O−N per kg NO_3^-−N (mean = 0.0028) compared to a value of 0.0025 kg N_2O−N per kg NO_3^-−N for IPCC.

DISCUSSION

Changes in NO_3^- concentrations have been shown to control N_2O in nitrogen-enriched rivers, streams, and estuaries.[13,39−41] In our study, NO_3^- was an important predictor of dissolved N_2O and flux chamber measurements of N_2O. Long-term trends show peak river flow at Site 116 between February and April and low flows, coupled with high NO_3^-, between August and September.[21] In 2011, the SJR Water Year Index (unimpaired flow at Site 116) was 170% above average, resulting in higher winter to early summer flows.[33] Rainfall in February significantly increased mean NO_3^-−N concentrations from the previous sampling event (January = 0.57 to February = 1.49 mg L^{-1}), especially at upstream sites, due to greater surface runoff and subsurface agricultural drainage. Kratzer et al. [21] estimated that NO_3^-−N from upstream of Site 212 can contribute up to 50% more NO_3^- during wet years. In contrast, high river flows in April 2011 from above-average Sierra Nevada snowmelt, rather than agriculture discharge, resulted in a decrease in NO_3^-−N concentrations (0.19 mg L^{-1}).

Dissolved N_2O concentrations in surface waters were in the range of values reported in previous studies on smaller streams and estuaries,[42,43] while N_2O saturation was relatively high compared to other studies on lakes (range = 112−209%[41,44]) and estuaries (range = 70−363%[43]), but lower than the average values in the Tama Estuary (mean = 586%) and River (mean = 1051%[45]) and the eutrophic Yangtze Delta (range = 175−4914%[46]). Flux chamber measurements of N_2O (range = 9.5−372 $\mu g\ m^{-2}\ hr^{-1}$) were higher than those reported by Beaulieu et al.[47] (mean = 12.2−16.2 $\mu g\ m^2\ hr^{-1}$) and Cole and Caraco[48] (mean = 6.3 $\mu g\ m^{-2}\ hr^{-1}$) on comparably large rivers.

Dissolved N_2O concentrations were best predicted by temperature and NO_3^- concentrations. It is well understood that denitrifying microbes respond to increases in temperature and NO_3^- availability.[49,50] The effects of temperature on N_2O concentrations are similar to those in a comparatively large river system from Beaulieu et al.,[47] but contradictory to Lui et al.,[11] who reported higher N_2O concentrations with lower temperatures in the Wujiang River.

Several indicators in this study suggest denitrification in shallow anoxic benthic sediments was the main process responsible for N_2O production. Within the river water column there were persistent oxic conditions, a lack of a relationship between NH_4^+ or DO with N_2O concentrations, and a strong relationship between NO_3^- and N_2O concentrations. Along the entire 118 km study reach, anoxic sediments were identified by iron reduction and removal or the presence of sulfides beginning at depths ranging from ∼5−10 cm beneath the water column−sediment interface.[22] The benthic sediments were composed of medium to coarse sands allowing for relatively rapid exchange of water between the water column and benthic sediments.[51] During the sediment-porewater sampling dates, the average NO_3^- concentrations in the top 2 cm were highest and decreased rapidly with depth at most sites (Table S1). This implies the high NO_3^- concentrations in the water column during the time of porewater sampling resulted in greater delivery of NO_3^- to the anoxic sediments of the hyporheic zone. In addition, sediment porewater O_2 concentrations were mostly <4 mg L^{-1} at Sites 201−160.

High NO_3^- concentrations can inhibit the reduction of N_2O to N_2 resulting in higher N_2O yields.[52,53] This has been demonstrated in agricultural soils[54,55] and riparian zones[56,57] but fewer studies have measured N_2O yield from denitrification in streams and rivers. Silvennoinen et al [40] found increases in NO_3^- load, which resulted in increases in both N_2 and N_2O to the water column. They found that N_2O contributed only 3.9% of total denitrification. In this study, the mean N_2O−N:NO_3^-−N ratio in surface waters was 0.002 with a maximum of 0.01. Whereas, the average N_2O−N:NO_3^-−N ratio in sediment-porewaters (0.043) was an order of magnitude higher than

surface waters. In sum, our data suggest that hyporheic sediments are a significant source of N_2O, produced by denitrification, receiving nitrate from the water column that mixes with the anoxic sediments.

Although there is strong support in the current study for denitrification as the main pathway for production of N_2O, other biological processes cannot be ruled out. The processes responsible for N_2O production include nitrification, coupled nitrification−denitrification, nitrifier denitrification, and dissimilatory nitrate reduction to ammonium (DNRA).[58−60] The IPCC assumes N_2O production by nitrification is twice as high as denitrification for lakes and rivers.[4] Nitrification has been shown to occur in the water column of streams with high suspended solids or diffusion from oxic sediment layers.[61,62] Although increases in turbidity have been associated with high flows in SJR,[63] a relationship between dissolved N_2O and NH_4^+ in surface waters was not found. Our range of NH_4^+ concentrations in the water column may have been too low to indicate the relative importance of N_2O formation by nitrification of NH_4^+. N_2O can be augmented by coupled nitrification−denitrification at the aerobic−anaerobic sediment interface. Ammonium concentrations in sediment-porewaters were greater at 18 and 30 cm compared to the 2 cm depth (Table S1). The elevated NH_4^+ (maximum = 48.5 N L^{-1}) was presumed to be formed by anaerobic mineralization.[22] As NH_4^+ transports upward entering more oxic water, nitrification is favorable, thus contributing to NO_3^- and potentially N_2O production. This was demonstrated in this study by the opposing fluctuation of NH_4^+ and NO_3^- concentrations with depth (Table S1). When oxygenated river water infiltrates within shallow benthic sediments, coupled nitrification and denitrification can contribute to N_2O production. N_2O concentrations in sediment-porewaters tended to be highest in the upper 18 cm of the sediment column that typically contained the oxic−anoxic transition zone. Thus as NH_4^+ diffuses upward, it can be nitrified to NO_3^-, which coupled with NO_3^- inputs from surface waters, creates a hot spot for dissolved N_2O production. Given the limited temporal and spatial sampling of porewater chemistry, further intense field studies are recommended to validate the current observations.

The chamber-measured N_2O fluxes were in good agreement with the model-estimated N_2O fluxes from Sites 201−160. Gas transfer velocities in large bodies of water are controlled by turbulence from wind, whereas in smaller streams turbulence is a function of water movement over sediments and transfer velocities are a function of river depth and velocity.[64] Various wind and benthic driven models have been proposed for calculating gas transfer velocities[65,66] and previous studies have found other parameters such as wind fetch and organic matter can contribute to gas transfer velocity.[67,68] Five alternative gas transfer velocity models were used to estimate N_2O fluxes and compare with the method used in this study.[66,69,70] The five models were chosen to compare gas transfer velocities based on wind-driven turbulence, water turbulence, and three methods using a combined wind and water turbulence to estimate N_2O gas fluxes (Section S7). The estimated fluxes showed variability among the five models (Figure S3). The variance among the different equations for estimated fluxes increased with increasing river size (Figure S3) and during May 2011, where wind speed was above 3.6 m s^{-1} (Figure S4). The efficiency of floating chambers has been debated due to effects of wind turbulence overestimating N_2O fluxes.[65,71] Paired *t* tests between measured N_2O fluxes and model-estimated fluxes were not significantly different except for eq 7 (Section S7), where the wind turbulence was not incorporated into the estimated fluxes. Using equations that did not use wind turbulence resulted in considerably lower estimated fluxes compared to measured fluxes. Likewise, without incorporating the effects of water turbulence (eq 5), estimated fluxes were lower than measured fluxes and the other estimated fluxes (eq 7−10) using the combined wind and water turbulence. On rivers such as the SJR that vary annually and between reaches, using a combined wind/water turbulence model produced the best fit with chamber-measured N_2O fluxes. As there was a large variation between models at high flow, in agreement with Raymond et al.,[66] caution should be used when modeling N_2O fluxes for larger rivers. Improving methods for accurately measuring and modeling N_2O emissions from high-order streams is critically needed.

Investigating diurnal variability in N_2O was beyond the scope of this study, although significant differences between water chemistry characteristics and dissolved N_2O concentrations were not found between 09:00 and 21:00 at Sites 144 and 94. Harrison et al.[10] found rates of N_2O production to be greatest during the day and minimal at night, whereas Baulch et al.[72] found inconsistent patterns of N_2O fluxes over 24 h. Rosamond et al.[73] found most of their sampling events demonstrated an increase in N_2O at night in association with decreased O_2 concentration, while some sampling events showed increases in N_2O in both day and nighttime. As previous studies on the SJR have recorded diurnal shifts in O_2 and NO_3^-, future research on N_2O in the SJR is necessary to verify the results of our diurnal investigation.[74,75]

Dissolved N_2O and NO_3^- concentrations measured in the SAC did not vary significantly over the duration of the study. A significant relationship between N_2O and NH_4^+ in the SAC suggests that nitrification may be a source of N_2O production. Previous studies have identified the Sacramento Regional Wastewater Treatment Plant as a significant contributor of NH_4^+ in the lower SAC.[51] This may contribute to increases in N_2O via nitrification in the water column during downstream transport. Pakulski et al.[76] observed a similar pattern in the Mississippi River with high NH_4^+ concentrations stimulating the occurrence of nitrification in the water column.

It is well documented that N removal is less efficient as river flow and depth increase during downstream transport.[77,78] This is due to a greater volume of water resulting in less contact between the water column NO_3^- and benthic sediments (i.e., decreased benthic sediment to water volume ratio) and lower hydrologic residence times. In many cases, hydrologic characteristics (i.e., discharge, depth, width) were found to be equally as important as biological characteristics.[79] In this study, NO_3^- residence time demonstrated a first-order inverse relationship with depth and flow (Table S1). This is consistent with previous studies on the physical parameters of nutrient transport downstream in streams and rivers.[80] Less is known about how hydrologic characteristics influence loss of N by N_2O fluxes during downstream transport. At Site 212, where the benthic surface area to water volume ratio was highest (range = 0.44−1.83, mean = 0.91), there was a greater N_2O−N:NO_3^-−N ratio (range = 0.00045−0.01). In addition, the dissolved N_2O−N:NO_3^-−N ratio from sediment-porewater in the top 8 cm at Site 201 (mean = 0.038) was ∼3 times higher than that in surface waters and any measured porewater from the other sites. When accounting for N_2O−N loss from each of the 9 river sections across all months, piecewise regression showed that N_2O−N was positively related to NO_3^-−N concentrations when river flow was less than 65 m^3 s^{-1}. Above this threshold, stepwise linear

dx.doi.org/10.1021/es301373h | Environ. Sci. Technol. 2013, 47, 1313−1322

regression showed that the width of the river was more important than NO_3^-–N, predicting 66% ($P < 0.004$) of total N loss as N_2O. This suggests loss of N_2O was more dependent on river hydrological influences, such as flow and benthic to water volume ratios, at higher flows.

To determine the magnitude of N_2O fluxes from the SJR, assessments of N loss as N_2O were compared to those estimated using the IPCC EF5 protocol. Estimated N loss as N_2O from the SJR were up to 3 times greater than those estimated using IPCC flux estimates of N_2O per kg NO_3^-–N. Clough et al.[12] and Baulch et al.[72] found comparable values with the 2007 IPCC EF5-r value modifications. The findings from this study suggest calculating the EF5-r using the IPCC protocol may be an oversimplified method when applied to high-order streams. Changing flow, turbulence, width/depth ratio, and hydraulic residence times will certainly have an influence on N_2O production rates over the course of a year. In agreement with Baulch et al.[81] and Clough et al.,[17] a revision to the IPCC EF5 factor with consideration of river hydrological characteristics may be warranted.

This study provides the first data on dissolved N_2O and fluxes for the eutrophic SJR. Results from this study suggest denitrification is the primary source of N_2O within the SJR. Moderately high N_2O fluxes compared to smaller streams and larger rivers highlight that SJR can be a significant source of indirect N_2O emissions. Guo et al.[82] modeled direct N_2O emissions from agricultural soils using the denitrification–decomposition (DNDC) model and estimated annual N_2O emissions from all agricultural fields in California was 1.27×10^4 Mg N with 83% located within the Central Valley. Specifically, annual N_2O emissions from San Joaquin County agricultural fields averaged 11.0 kg N ha^{-1} yr^{-1} and accounted for 11% of the total N_2O emissions from California agricultural fields. Comparatively, N_2O–N emissions from the SJR wetted surface area were 5.7 kg N ha^{-1} yr^{-1}. This emphasizes the critical need to improve management efforts to reduce NO_3^- loading in the SJR. Additionally, results from the study illustrate the potential for other N_2O generating processes such as nitrification and indirectly, production of NH_4^+ by anaerobic mineralization. As there is currently a lack of information on N_2O within the SJR, further research should focus on estimating emissions in addition to N_2O production by denitrification and nitrification potential from water column and benthic sediments.

■ ASSOCIATED CONTENT

Supporting Information

Additional information on the alternative gas transfer velocity models, ancillary data, and figures on sediment-porewater depth profile and model-estimates of N_2O. This material is available free of charge via the Internet at http://pubs.acs.org.

■ AUTHOR INFORMATION

Corresponding Author

*Phone: 815-409-5816; e-mail: sarra.hinshaw@gmail.com.

Notes

The authors declare no competing financial interest.

■ ACKNOWLEDGMENTS

This project was supported by the U.S. Bureau of Reclamation. We thank Xien Wang for laboratory assistance and Kim Mark, Diana Cabrera, and Dr. Chen Dingjiang for assisting in the field experiments.

■ REFERENCES

(1) Forster, P. Changes in atmospheric constituents and in radiative forcing. In *Climate Change 2007: The physical science basis. Contributions of Working Group I to the Fourth Assessment Report of the Intergovernmental Panel on Climate Change*; Solomon, S., Qin, D., Manning, M., Marquis, M., Averyt, K., Tignor, M. M. B., Henry LeRoy Miller, J., Chen, Z., Eds.; Cambridge University Press: Cambridge, United Kingdom and New York, 2007.

(2) Syakila, A.; Kroeze, C. The global nitrous oxide budget revisited. *GHGMM* **2011**, *1* (1), 17–26.

(3) Zaehle, S.; Ciais, P.; Friend, A. D.; Prieur, V. Carbon benefits of anthropogenic reactive nitrogen offset by nitrous oxide emissions. *Nat. Geo* **2011**, *4*, 601–605.

(4) IPCC. *2006 IPCC Guidelines for National Greenhouse Gas Inventories*; Eggleston, H. A., Buendia, L. Miwa, K., Ngara, T. Tanabe, K., Eds.; Prepared by the National Greenhouse Gas Inventories Programme; IGES: Japan, 2006.

(5) IPCC. *Guidelines for National Greenhouse Gas Inventories*; OECD/OCDE: Paris, 1997.

(6) Hiscock, K. M.; Bateman, A. S.; Muhlherr, I. H.; Fukada, T.; Dennis, P. F. Indirect emissions of nitrous oxide from regional aquifers in the United Kingdom. *Environ. Sci. Technol.* **2003**, *37*, 3507–3512.

(7) Reay, D. S.; Smith, K. A.; Edwards, A. C. Nitrous oxide in agricultural drainage waters following field fertilisation. *Water, Air, Soil Pollut.* **2004**, *4*, 437–451.

(8) Sawamoto, T.; Nakajima, Y.; Kasuya, M.; Tsuruta, H.; Yagi, K. Evaluation of emission factors for indirect N_2O emission due to nitrogen leaching in agro-ecosystems. *Geophys. Res. Lett.* **2005**, *32*, (L03403) DOI: 10.1029/2004GL021625.

(9) Garnier, J.; Billen, G.; Vilain, G.; Martinez, A.; Silvestre, M.; Mounier, E.; Toche, F. Nitrous oxide (N_2O) in the Seine river and basin: Observations and budgets. *Agric. Ecosyst. Environ.* **2009**, *133* (3–4), 223–233.

(10) Walker, J. T.; Stow, C. A.; Geron, C. Nitrous oxide emissions from the Gulf of Mexico hypoxic zone. *Environ. Sci. Technol.* **2010**, *44*, 1617–1623.

(11) Liu, X. L.; Liu, C. Q.; Li, S. L.; Wang, F. S.; Wang, B. L.; Wang, Z. L. Spatiotemporal variations of nitrous oxide (N_2O) emissions from two reservoirs in SW China. *Atmos. Environ.* **2011**, *45* (31), 5458–5468.

(12) Clough, T. J.; Buckthought, L. E.; Casciotti, K. L.; Kelliher, F. M.; Jones, P. K. Nitrous oxide dynamics in a braided river system, New Zealand. *J. Environ. Qual.* **2011**, *40*, 1532–1541.

(13) Beaulieu, J. J.; Arango, C. P.; Hamilton, S. K.; Tank, J. L. The production and emission of nitrous oxide from headwater streams in the Midwestern United States. *Global Change Biol.* **2008**, *14*, 1–17.

(14) Harrison, J. A.; Matson, P. A.; Fendorf, S. E. Effects of diel oxygen cycle on nitrogen transformations and greenhouse gas emissions in a eutrophied subtropical stream. *Aquat. Sci.* **2005**, *67*, 308–315.

(15) Wilcock, R. J.; Sorrell, B. K. Emissions of greenhouse gases CH_4 and N_2O from low-gradient streams in agriculturally developed catchments. *Water, Air, Soil Pollut.* **2008**, *188*, 155–170.

(16) Silvennoinen, H.; Liikanen, A.; Rintala, J.; Martikainen, P. Greenhouse gas fluxes from the eutrophic Temmesjoki River and its Estuary in the Liminganlahti Bay (the Baltic Sea). *Biogeochemistry* **2008**, *90* (2), 193–208.

(17) Clough, T. J.; Buckthought, L. E.; Kelliher, F. M.; Sherlock, R. R. Diurnal fluctuations of dissolved nitrous oxide (N_2O) concentrations and estimates of N_2O emissions from a spring-fed river: Implications for IPCC methodology. *Global Change Biol.* **2007**, *13* (5), 1016–1027.

(18) Beaulieu, J. J.; Tank, J. L.; Hamilton, S. K.; et al. Nitrous oxide emission from denitrification in stream and river networks. *Proc. Natl. Acad. Sci., U. S. A.* **2010**, *108* (1), 214–219.

(19) Seitzinger, S. P.; Kroeze, C.; Styles, R. V. Global distribution of N_2O emission from aquatic systems: Natural emission and anthropogenic effects. *Chemosphere: Global Change Sci.* **2000**, *2*, 267–279.

(20) Knowles, R. Denitrification. *Microbiol. Rev.* **1982**, *46*, 43–70.

(21) Kratzer, C.; Dileanis, P. D.; Zamora, C.; Silva, S. R.; Kendall, C.; Bergamaschi, B. A.; Dahlgren, R. A. *Sources and Transport of Nutrients, Organic Carbon, and Chlorophyll-a in the San Joaquin River*; U.S. Geological Survey: Sacramento, CA, 2004.
(22) Zamora, C.; Dahlgren, R. A.; Kratzer, C. R.; Downing, B. D.; Russell, A. D.; Dileanis, P. D.; Bergamaschi, B. A.; Phillips, S. P. *Groundwater Contributions of Flow, Nitrate, and Dissolved Organic Carbon to the Lower San Joaquin River, California, during 2006−2008*; U.S. Geological Survey: Reston, VA, 2012.
(23) LeLand, H. V.; Brown, L. R.; Mueller, D. K. Distribution of algae in the San Joaquin River, California, in relation to nutrient supply, salinity, and other environmental factors. *Freshwater Biol.* **2001**, *46*, 1136−1167.
(24) Saleh, D. K.; Domagalski, J. L,; Kratzer, C. R.; Knifong, D. L. *Organic Carbon Trends, Loads, and Yields to the Sacramento-San Joaquin Delta, California, Water Years 1980−2000*; U.S. Geological Survey: Sacramento, CA, 2003.
(25) City of Modesto. *Northern San Joaquin Valley Water Reclamation Project*; Vol. *1*, Feasibility Study Report; Modesto, CA, 2005.
(26) Dalsgaard, T. *Protocol Handbook for NICE: Nitrogen Cycling in Estuaries: A Project under the EU Research Programme Marine Science and Technology (MAST III)*; National Environmental Research Institute: Denmark, 2000.
(27) Weiss, R. F.; Price, B. A. Nitrous oxide solubility in water and seawater. *Mar. Chem.* **1980**, *8*, 347−359.
(28) Minami, K.; Fukushi, S. Methods for measuring N_2O flux from water surface and N_2O dissolved in water from agricultural land. *Soil Sci. Plant Nutr.* **1984**, *30*, 495−502.
(29) Wanninkhof, R. Relationship between wind speed and gas exchange over the ocean. *J. Geophys. Res.* **1992**, *97*, 7373−7382.
(30) Jahne, B.; Heinz, G.; Dietrich, W. Measurement of the diffusion coefficients of sparingly soluble gases in water. *J. Geophys. Res.* **1987**, *92*, 10767−10776.
(31) Puckett, L. J. Hydrogeologic controls on the transport and fate of nitrate in ground water beneath riparian zones: Results from thirteen studies across the United States. *Water Sci. Technol.* **2004**, *49*, 47−53.
(32) California Irrigation Management Information System. CIMIS. http://www.cimis.water.ca.gov, 2011.
(33) California Data Exchange Center. CDEC. http://cdec.water.ca.gov, 2011.
(34) Brown, R. *Data Analysis Framework Report: San Joaquin River Flow and Water Quality Data Atlas for 2005*; Jones and Stokes: Sacramento, CA, 2007.
(35) Doane, T. A.; Howarth, R. W. Spectrophotometric determination of nitrate with a single reagent. *Anal. Lett.* **2003**, *36*, 2713−2722.
(36) Forster, J. C. *Methods in Applied Soil Microbiology and Biochemistry*; Academic Press: UK, 1995.
(37) Underwood, A. J. Experiments in ecology and management: Their logics, functions and interpretations. *Aust. J. Ecol.* **1990**, *15*, 365−389.
(38) SPSS. *SPSS for Windows: Version 14*; Chicago, IL, 2001.
(39) Robinson, A. D.; Nedwell, D. B.; Harrison, R. M.; Ogilvie, B. J. Hypernutrified estuaries as sources of N_2O emission to the atmosphere: The estuary of the River Colne, Essex, UK. *Mar. Ecol.: Prog. Ser.* **1998**, *169*, 59−71.
(40) Silvennoinen, H.; Liikanen, A.; Torssonen, J.; Florian Stange, C.; Martikainen, P. Denitrification and nitrous oxide effluxes in boreal, eutrophic river sediments under increasing nitrate load: A laboratory microcosm study. *Biogeochemistry* **2008**, *91*, 105−116.
(41) McCrackin, M. L.; Elser, J. J. Atmospheric nitrogen deposition influences denitrification and nitrous oxide production in lakes. *Ecology* **2010**, *91* (2), 528−539.
(42) Clough, T.; Bertram, J. E.; Sherlock, R. R.; Leonard, R. L.; Nowicki, B. L. Comparison of measured and EF5-r-derived N_2O fluxes from a spring-fed river. *Global Change Biol.* **2006**, *12*, 477−488.
(43) Zhang, G. L.; Zhang, J.; Liu, S. M.; J. L., R.; Zhao, Y. C. Nitrous oxide in the Changjiang (Yangtze River) Estuary and its adjacent marine area: Riverine input, sediment release and atmospheric fluxes. *Biogeosciences* **2010**, *7*, 3505−3516.
(44) Huttunen, J. T.; Valsanen, T. S.; Heikkinen, M.; Hellsten, S.; Nykanen, H.; Nenonen, O.; Martikainen, P. J. Exchange of CO_2, CH_4 and N_2O between the atmosphere and two northern boreal ponds with catchments dominated by peatlands or forests. *Plant Soil* **2002**, *242*, 137−146.
(45) Toyoda, S.; Iwai, H.; Koba, K.; Yoshida, N. Isotopomeric analysis of N_2O dissolved in a river in the Tokyo metropolitan area. *Rapid Commun. Mass Spectrom.* **2009**, *23* (6), 809−821.
(46) Wang, D.; Chen, Z.; Sun, W.; Hu, B.; Xu, S. Methane and nitrous oxide concentration and emission flux of Yangtze Delta plain river net. *Sci. China, Ser. B: Chem.* **2009**, *52* (5), 652−661.
(47) Beaulieu, J. J.; Shuster, W. D.; Rebholz, J. A. Nitrous oxide emissions from a large, impounded river: The Ohio River. *Environ. Sci. Technol.* **2010**, *44* (19), 7527−7533.
(48) Cole, J. J.; Caraco, N. F. Emissions of nitrous oxide (N_2O) from a tidal, freshwater river, the Hudson River, New York. *Environ. Sci. Technol.* **2001**, *35*, 991−996.
(49) Jordan, T. E.; Weller, D. E.; Correll, D. L. Denitrification in surface soils of a riparian forest: Effects of water, nitrate and sucrose additions. *Soil Biol. Biochem.* **1998**, *30* (7), 833−843.
(50) Pfenning, K. S.; McMahon, P. B. Effect of nitrate, organic carbon, and temperature on potential denitrification rates in nitrate-rich riverbed sediments. *J. Hydrol.* **1997**, *187* (3−4), 283−295.
(51) Lee, G. F.; Jones-Lee, A. *Issues in Developing the San Joaquin River Deep Water Ship Channel DO TMDL. El Macero, CA*; Central Valley Regional Water Quality Control Board: Sacramento, CA, 2000.
(52) Firestone, M. K.; Firestone, R. B.; Tiedje, J. M. Nitrous oxide for soil denitrification: Factors controlling its biological production. *Science* **1980**, *208*, 749−751.
(53) Weier, K. L.; Doran, J. W.; Power, J. F.; Walters, D. T. Denitrification and dinitrogen/nitrous oxide ratio as affected by soil water, available carbon, and nitrate. *Soil Sci. Soc. Am. J.* **1993**, *57*, 66−72.
(54) Dalal, R. C.; Wang, W.; Robertson, G. P.; Parton, W. J. Nitrous oxide emission from Australian agricultural lands and mitigation options; a review. *Aust. J. Soil Res.* **2003**, *41*, 165−195.
(55) Schlesinger, W. H. On the fate of anthropogenic nitrogen. *Proc. Natl. Acad. Sci.* **2009**, *106*, 203−208.
(56) Hefting, M. M.; Bobbink, R.; Caluwe, H. D. Nitrous oxide emission and denitrification in chronically nitrate-loaded riparian buffer zones. *J. Environ. Qual.* **2002**, *32*, 1194−1204.
(57) Hunt, P. G.; Matheny, T. A.; Ro, K. S. Nitrous oxide accumulation in soils from riparian buffers of a coastal plain watershed-carbon/nitrogen ratio control. *J. Environ. Qual.* **2007**, *36*, 1368−1376.
(58) Wrage, N.; Velthof, G. L.; Laanbroek, H. J.; Oenama, O. Nitrous oxide production in grassland soils: Assessing the contribution of nitrifier denitrification. *Soil Biol. Biochem.* **2004**, *36*, 229−236.
(59) Rutting, T.; Boechx, P.; Muller, C.; Klemedtsson, L. Assessment of the importance of dissimilatory nitrate reduction to ammonium for the terrestrial nitrogen cycle. *Biogeosci. Discuss.* **2011**, *8*, 1169−1196.
(60) Smith, M. S.; Zimmerman, K. Nitrous oxide production by non-denitrifying soil nitrate reducers. *Soil Sci. Soc. Am. J.* **1981**, *45*, 865−871.
(61) Chesterikoff, A.; Garban, B.; Billen, G.; Poulin, M. Inorganic nitrogen dynamics in the River Seine downstream from Paris (France). *Biogeochemistry* **1992**, *17* (3), 147−164.
(62) Rysgaard, S.; Risgaard-Petersen, N.; Sloth, N. P.; Jensen, K.; Nielsen, L. P. Oxygen regulation of nitrification and denitrification in sediments. *Limnol. Oceanogr.* **1994**, *39* (7), 1643−1652.
(63) Jones and Stokes. *City of Stockton Year 2001 Field Sampling Program. Data Summary Report. San Joaquin River Dissolved Oxygen TMDL;* Sacramento, CA, 2002.
(64) Raymond, P. A.; Cole, J. J. Gas exchange in rivers and estuaries: Choosing a gas transfer velocity. *Estuaries* **2001**, *24*, 312−317.
(65) Zappa, C. J.; McGillis, W. R.; Raymond, P. A.; Edson, J. B.; Hintsa, E. J.; Zemmelink, H. J.; Dacey, J. W. H.; Ho, D. T.

Environmental turbulent mixing controls on air-water gas exchange in marine and aquatic systems. *Geophys. Res. Lett.* **2007**, *34* (10), L10601.
(66) Raymond, P. A.; Zappa, C. J.; Butman, D.; Bott, T. L.; Potter, J.; Mulholland, P.; Laursen, A. E.; McDowell, W. H.; Newbold, D. Scaling the gas transfer velocity and hydraulic geometry in streams and small rivers. *Limnol. Oceanogr. Fluid Eng.* **2012**, *2*, 41−53.
(67) Guerin, F.; Abril, G.; Serca, D.; Delon, C.; Richard, S.; Delmas, R.; Tremblay, A.; Varfalvy, L. Gas transfer velocities of CO_2 and CH_4 in a tropical reservoir and its river downstream. *J. Mar. Syst.* **2007**, *66*, 161−172.
(68) Harrison, E. L.; Veron, F.; Ho, D. T.; Reid, M. C.; Orton, P.; McGillis, W. R. Nonlinear interaction between rain-and wind-induced air-water gas exchange. *J. Geophys. Res* **2012**, 117 DOI: 10.1029/2011JC007693.
(69) Nightingale, P.; Malin, G.; Law, C. S.; Watson, A. J.; Liss, P. S.; Liddicoat, M. I.; Bouting, J.; Upstill-Goddard, R. C. In-situ evaluation of air-sea gas exchange parameterizations using novel conservative and volatile tracers. *Global Biogeochem. Cycles* **2000**, *4*, 373−387.
(70) Borges, A. V.; Vanderborght, J. P.; Schiettecatte, L. S.; Gazeau, F.; Ferron-Smith, S.; Delille, B.; Frankignoulle, M. Variability of the gas transfer velocity of CO_2 in a macrotidal estuary (the Scheldt). *Estuaries* **2004**, *27* (4), 593−603.
(71) Crusius, J.; Wanninkhof, R. Gas transfer velocities measured at low wind speed over a lake. *Limnol. Oceanogr.* **2003**, *48* (3), 1010−1017.
(72) Baulch, H. M.; Dillion, P. J.; Maranger, R.; Venkiteswaran, J. J.; Wilson, H. F.; Schiff, S. L. Night and day: Short-term variation in nitrogen chemistry and nitrous oxide emissions from streams. *Freshwater Biol.* **2012**, *57*, 509−525.
(73) Rosamond, M. S.; Thuss, S. J.; Schiff, S. L.; Elgood, R. J. Coupled cycles of dissolved O_2 and N_2O in rivers along a trophic Gradient, Southern Ontario, Canada. *J. Environ. Qual.* **2011**, *40*, 256−270.
(74) Pellerin, B. A.; Downing, B. D.; Kendall, C.; Dahlgren, R. A.; Kraus, T. E. C.; Saraceno, J.; Spencer, R. G. M.; Bergamaschi, B. A. Assessing the sources and magnitude of diurnal nitrate variability in the San Joaquin River (California) with an in situ optical nitrate sensor and dual nitrate isotopes. *Freshwater Biol.* **2009**, *54* (2), 376−387.
(75) Volkmar, E. C.; Henson, S. S.; Dahlgren, R. A.; O'Geen, A. T.; Van Nieuwenhuyse, E. E. Diel patterns of algae and water quality constituents in the San Joaquin River, California, USA. *Chem. Geol.* **2011**, *283*, 56−67.
(76) Pakulski, J. D.; Benner, R.; Whitledge, T.; Amon, R.; Eadie, B.; Cifuentes, L.; Ammerman, J.; Stockwell, D. Microbial metabolism and nutrient cycling in the Mississippi and Atchafalaya River plumes. *Estuarine Coastal Shelf Sci.* **2000**, *50*, 173−184.
(77) Alexander, R. B.; Smith, R. A.; Schwarz, G. E. Effect of stream channel size on the delivery of nitrogen to the Gulf of Mexico. *Nature* **2000**, *403*, 758−761.
(78) Donner, S. D.; Kucharik, C. J.; Oppenheimer, M. The influence of climate on in-stream removal of nitrogen. *Geophys. Res. Lett.* **2004**, *31*, (L20509) DOI: 10.1029/2004GL020477.
(79) Muholland, P. J.; Helton, A. M.; Poole, G. C.; et al. Stream denitrification across biomes and its response to anthropogenic nitrate loading. *Nature* **2008**, *452*, 202−205.
(80) Alexander, R. B.; Böhlke, J. K.; Boyer, E. W.; David, M. B.; Harvey, J. W.; Mulholland, P. J.; Seitzinger, S. P.; Tobias, C. R.; Tonitto, C.; Wollheim, W. M. Dynamic modeling of nitrogen losses in river networks unravels the coupled effects of hydrological and biogeochemical processes. *Biogeochemistry* **2009**, *93*, 91−116.
(81) Baulch, H. M.; Schiff, S. L.; Maranger, R.; Dillon, P. J. Testing models of aquatic N_2O flux for inland waters. *Can. J. Fish. Aquat. Sci.* **2012**, *69*, 145−160.
(82) Guo, L.; Luo, D.; Li, C.; FitzGibbon, M. Development of spatial inventory of nitrous oxide emissions from agricultural land uses in California using biogeochemical modeling. In *Understanding Greenhouse Gas Emissions from Agricultural Management*; Guo, L., Gunasekara, A., McConnell, L., Eds.; ACS Symposium Series, Vol. *1072*, 2011; pp 387−403.